THE JOURNAL OF PHYSICAL CHEMISTRY B

Article

pubs.acs.org/JPCB

Condensation, Complex Coacervation, and Overcharging during DNA−Gelatin Interactions in Aqueous Solutions

Najmul Arfin and H. B. Bohidar*

Polymer and Biophysics Laboratory, School of Physical Sciences, Jawaharlal Nehru University, New Delhi-110067, India

Supporting Information

ABSTRACT: Interaction between DNA (effective hydrodynamic radius, $R_{DNA} \approx 140$ nm) and Gelatin A (GA) (effective hydrodynamic radius, $R_{GA} \approx 55$ nm) with charge ratio (DNA:GA = 16:1) and persistence length ratio (5:1) was studied by using fixed DNA concentration (5×10^{-3} % (w/v)) and varying GA concentration (C_{GA} = 0−0.25% (w/v)). Experimentally, three interesting regions of interaction were observed from dynamic light scattering, turbidity, zeta potential, and viscosity data: (i) $C_{GA} < 0.05\%$ (w/v), GA binds to DNA forming soluble complexes of size $R_{complex} \approx 60$ nm < R_{DNA} (primary binding causing condensation); (ii) $0.05\% < C_{GA} < 0.1\%$ (w/v), $R_{complex} \approx 60$ to 180 nm was observed up to charge-neutralization point (secondary binding); and (iii) $C_{GA} > 0.1\%$ (w/v) showed interesting overcharging behavior of DNA−GA complexes, followed by liquid−liquid phase separation (complex coacervation). Aforesaid regions of interaction were further examined theoretically by modeling the problem using electrostatic and van der Waals interaction potentials treating GA molecules as counterions to DNA macroion. Region (i) was explained on the basis of electrostatic screening, followed by reduction in persistence length, which resulted in condensation of DNA−GA complex. In region (ii), the dominance of van der Waals forces led to the formation of large soluble complexes through selective binding. This was possible due to closer proximity between GA and DNA−GA complexes and the absence of strong electrostatic forces. In region (iii), these oversized and overcharged complexes coarsened, leading to complex coacervation. Here the interaction energy profile showed that a greater number of counterions was required over and above the usual charge neutralization requirement for low-energy configurations to be achieved.

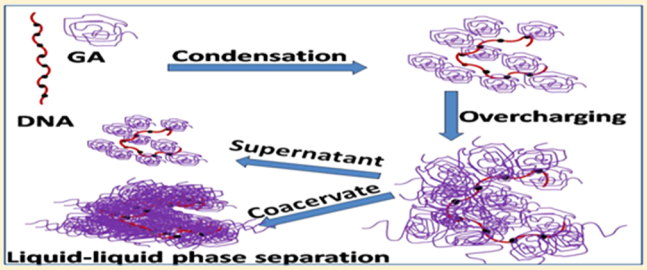

1. INTRODUCTION

Intermolecular associative interaction between oppositely charged macromolecules, which is mostly driven by electrostatic forces, often leads to liquid−liquid phase separation (called coacervation transition). Coacervation is usually defined as the spontaneous formation of a super dense liquid phase from a homogeneous macromolecular solution of poor solvent affinity.[1] Here a homogeneous solution separates into a polymer-rich phase (called coacervate) and its supernatant.[2] In complex coacervation, the loss of solvation that lead to phase separation arises from the interaction of complementary macromolecular species. The formation of such macromolecule-rich fluids is well known in mixtures of complementary polyelectrolytes.[3] It also occurs from mixtures of polyelectrolytes with colloidal particles, leading to condensed phases that are associated with interesting properties. Coacervation has been observed in a wide range of polyelectrolyte systems, like poly(dimethyldiallylammonium chloride)-bovine serum albumin,[4] gelatin-chitosan,[5] gelatin-agar,[6,7] gelatin−gelatin,[8,9] and so on. In addition, experiments that explored the formation of similar self-organized microscopic structures using nucleic acids were highly successful.[10]

Binding of DNA to proteins[11,12] and oppositely charged spherical macroions[13] has revealed interesting results. Mrevlishvili and Svintradze[11] have reported interaction between worm-like chains of DNA duplex of persistence length 50 nm, contour length 3000 nm, and width 2 nm with collagen rod-like structures of length 300 nm and width 1.5 nm. The DNA−collagen complex was found to have overlapped hydration shells of the two structures that yielded destruction of collagen triple helix and stabilization of DNA duplex. This self-assembled supramolecular structure can increase the stability of DNA against nucleases[14] and inhibit the excessive fibrillogenesis of native collagen in the presence of DNA.[15] Kaya et al.[12] compared the relative binding between ss-DNA and ds-DNA complexes with collagen and concluded that the structure of fibrils formed in the complexes showed remarkable dependence on DNA form. Nguyen and Shklovskii[13] examined the phase diagram of DNA and positively charged colloidal macroions in dispersion and observed the following: (i) at low colloid concentration, the DNA−colloid complexes are negatively charged with DNA wrapping the colloids, whereas (ii) at high colloid concentration, the complexes showed charge reversal and revealed positive charge. The aforesaid two situations are separated by an intermediate phase where the complexes are fully charge-neutralized; here

Received: July 26, 2012
Revised: October 16, 2012
Published: October 16, 2012

DNA−colloid condensates exist. Therefore, the concentration of colloidal macroions governed the condensation and reentrant condensation in this system. In a further extension of their work, the same group[16] studied the phase diagram of DNA and polycation (PC) and observed that the complex charge state was decided by the DNA/PC charge ratio. In this study, the existence of overcharged intermolecular complexes was clearly proposed. Gurovitch and Sens[17] proposed an idealized model for the adsorption of weakly charged polyelectrolyte onto oppositely charged colloidal particles. They applied self-consistent field theory and showed that the connectivity between the charges of the polymer leads to overcharging of the colloid. Their calculation revealed that each colloid particle could adsorb a chain segment carrying a total charge that was 15/6 times its own charge.

Proteins can interact with DNA either specifically or nonspecifically. In the case of nonspecific interactions, the sequences of nucleotides do not matter as far as the binding interactions are concerned. Histone (protein)−DNA interactions are an example of such interactions, and they occur between functional groups on the protein and the sugar−phosphate backbone of DNA. Specific DNA−protein interactions, however, depend on the sequence of bases in the DNA and on the orientation of the bases that can vary with twisting and supercoiling. These DNA−protein interactions are strong and are mediated by: (i) Hydrogen bonding mediated by water molecules, (ii) ionic interactions like formation of salt bridges, protein side chains−DNA backbone interaction, and (iii) van der Waals and hydrophobic interactions. Such interactions can produce novel biomaterials, and investigation of such systems aids to our general understanding of soft matter.

Herein we report a detailed study that probed the interaction between a low-charge-density polypeptide (gelatin A) and 200-base-pair DNA in salt-free aqueous solutions at room temperature (25 °C). The binding profile indicated the following dependence on protein concentration: DNA condensation (C_{GA} < 0.05% (w/v)), formation and growth of DNA−GA complexes (0.05 < C_{GA} < 0.1% (w/v)), and finally formation of overcharged intermolecular soluble complexes, followed by complex coacervation (C_{GA} > 0.1% (w/v)).

2. MATERIALS AND METHODS

Gelatin A (300 bloom) from porcine skin (nominal M_w = 100 kDa) and DNA (nominal M_w = 50−100 KDa) was procured from Sigma-Aldrich Chemicals and Acros Organics, respectively, and used as received. Stock of Gelatin A solution was prepared by dissolving a known amount of the protein in double-distilled deionized water at 40 °C using a magnetic stirrer for almost 2 h. DNA stock was prepared by dissolving DNA powder in double-distilled deionized water at room temperature for 1 h. Both solutions appeared optically clear and transparent after preparation. Final samples for experiment were prepared by mixing Gelatin A and DNA solution from their stock, and appropriate dilution was used to achieve exact mixing ratios. In all of the stock solutions, DNA concentration was maintained at 0.005% (w/v), whereas Gelatin A concentration was varied from C_{GA} = 0 to 0.25% (w/v). These samples were stored in airtight borosilicate glass tubes for further analysis, which, in all instances, did not exceed more than 48 h after preparation. All procedures were performed at room temperature, 25 °C, and relative humidity in the room was close to 50%.

The solution viscosity, η, and intrinsic viscosity, $[\eta]$, of samples were measured using a vibro viscometer (model-SV10, A&D, Japan). This instrument uses a matched pair of gold-plated flat electrodes. The mechanical vibrations (frequency ∼30 Hz) set in one of these propagate through the sample and are picked up by the other electrode. With this technique, the product of the viscosity and density is directly measured. With such low frequency and dilute concentration of sample, shear rate effects are negligible and density can be assumed to be constant. DLS experiments of the sample solution were performed at scattering angle of θ = 90° and laser wavelength of λ = 632.8 nm using commercial DLS instrument Rina (Nabitech, Germany) that was operated in the multi-τ mode (logarithmically spaced channels). The instrument was placed on a Newport (USA) vibration isolation table. In this method, the system has refractive index n and is physically seen over a length scale q^{-1}, where $q = (4\pi n/\lambda)$ sin $\theta/2$. The laser wavelength in the scattering medium is λ/n, where n is index of refraction. The diffusion coefficient for spherical particle having low Reynold number is related to a corresponding hydrodynamic radius through the Stoke−Einstein relation[18] as

$$D = K_B T/(6\pi\eta_0 R_H) \quad (1)$$

where solvent viscosity is η_0, K_B is Boltzmann constant, and T is absolute temperature. The zeta potential measurements of sample solution were performed on an electrophoresis instrument (ZC-2000, Microtek, Japan). The zeta potential, ζ, of a uniformly charged sphere is given by $\zeta = 4\pi\sigma/\varepsilon\kappa$, where σ is the surface charge density of the particle and ε and κ are the dielectric constant and the Debye−Huckel parameter of the solution, respectively. The extent of intermolecular interaction was estimated through quantitative measurement of solution turbidity. The change in transmittance (%T) was monitored continuously using a colorimeter (Brinkmann-910, Brinkmann Instruments, U.S.) operating at 450 nm.

3. RESULTS AND DISCUSSION

3.1. Characterization of DNA and Gelatin A. It was felt imperative to characterize physically the biopolymers used prior to undertaking the binding behavior study. The molecular weight of Gelatin A and base-pair quantification of DNA were performed using SDS-PAGE and agarose gel electrophoresis methods. The gel column pictures are consigned to the Supporting Information (Figures S1 and S2).

(a). SDS-PAGE and Western Blotting. SDS-PAGE was carried according to Laemmli's method (Laemmli, 1970). Western blotting was performed by transfer of protein separated in SDS-PAGE, transferred to PVDF (polyvinylidene difluoride) membrane using semidry transfer system (BioRad) according to standard protocol. In the transfer buffer SDS was included to increase transfer efficiency of high-molecular-weight proteins. Membrane was blocked with 5% Bloto (Genotech, USA) in TBST for 1h. Protein bands were probed with respective antiserum, washed with TBST, incubated with 1:10 000 dilution of HRP-conjugated secondary antibody (BioRad). and detected with enhanced chemiluminescence's (ECL) method. Protein gels were stained in staining solution (45% methanol, 10% acetic acid. and 0.25 g Coomassie dye) and destained in destaining solution (45% methanol, 10% acetic acid) overnight to remove the Coomassie dye. This study attributed a molecular weight 90 ± 10 KD to GA.

(b). Agarose Gel Electrophoresis. Agarose gel electrophoresis was performed as described by Sambrook et al., 1989. For plasmid DNA samples, 1% agarose was prepared in 1× TAE [40

mM Tris-Acetate, 1.0 mM EDTA (pH 8.0)] buffer by heating and cooled to 45 °C, and ethidium bromide (0.5 μg/mL) was added to stain the gel. DNA samples were mixed with one-sixth volume of DNA gel loading buffer and loaded onto the wells. Electrophoresis was performed at 5 V/cm in TAE buffer (40 mM Tris-Acetate, 1.0 mM EDTA, pH 8.0), and DNA samples were visualized on an UV transilluminator at 302 nm. The number of base pairs estimated was 200 for our sample.

(c). Persistence Length of DNA and Gelatin A. Persistence length (l_p) is the average projection of the end-to-end vector on the tangent to the chain contour at a chain end in the limit of infinite chain length or the integral of the average projections of chain elements of the infinitely long chain on its initial direction.[19] It is a measure of stiffness of the polymer. It is an intrinsic property of a polymer molecule. For polyelectrolytes, $l_p = (l_o + l_e)$, where l_o and l_e are bare and electrostatic persistence lengths. The latter is a function of solution ionic strength and polyelectrolyte charge density. Benoit and Doty[20] have derived the following expression relating the unperturbed radius of gyration (R_g) to l_p and the contour length (L_m).[20]

$$(R_g^2)/(l_p^2) = L_m/3l_p - 1 + 2l_p/L_m - 2L_m^2/l_p\{1 - \exp(-L_m/l_p)\} \quad (2)$$

which can be approximated to eq 3 if $L_m \gg l_p$

$$l_p = 3(R_g^2)/L_m \quad (3)$$

For spherical particles, $R_g^2 = (3/5)R_h^2$, which gives $l_p = (9/5)R_h^2/L_m$ yielding $l_p \approx 10.3$ nm for GA and $l_p \simeq 50$ nm for DNA, taken from literature.[11,21]

3.2. DNA–GA Binding Profile. The DNA solution was titrated with Gelatin A (GA) solutions under mild stirring, solution turbidity and viscosity, and ζ potential, and hydrodynamic radii of the DNA–GA complexes formed were monitored continuously. Figure 1 depicts these data clearly, which is quite revealing. The binding profile has three distinguishable regions of interaction of DNA with GA: (i) In the first region, which ends at C_{GA} = 0.05% (w/v), the turbidity increase was marginal (<10%), ζ potential decreased from −70 to −60 mV (25%), and hydrodynamic radii decreased by close to 50%. (ii) Significant change in solution properties was observed for 0.05 < C_{GA} < 0.1% (w/v), the turbidity increased five-fold, the ζ potential decreased from −50 mV to zero (complete charge neutralization), and hydrodynamic radii increased two-fold. (iii) For C_{GA} > 0.1% (w/v), the complexes were found to be positively charged (overcharging), turbidity decreased sharply, and so did the complex size, leading to liquid–liquid phase separation.

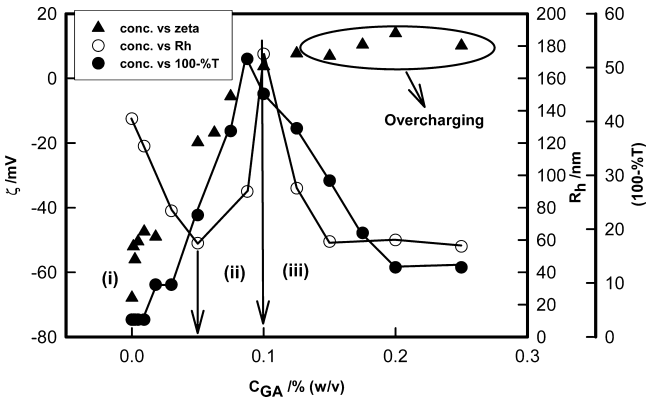

Figure 1. Variation of hydrodynamic radii, zeta potential of DNA–GA complex, and solution turbidity at different GA concentrations in region (i) condensation, primary binding (ii) secondary binding (iii) overcharging and complex coacervation. DNA concentration was fixed at 0.005% (w/v). %*T* is the percentage transmission of light from sample solution in turbidity experiment. Experimental data pertain to 25 °C. Solid lines are guide to eye.

3.3. Condensation of DNA (C_{GA} < 0.05% (w/v)). The addition of multivalent counterions and nonsolvents is known to condense DNA molecules.[22,23] However, an oppositely charged polymer can very easily be taken as a compacting agent, and for that complete charge neutralization is not necessary. Here the pH of the DNA, GA, and the mixed solutions was close to 6.0 ± 0.5. At this pH, the ζ potential of DNA and GA was measured to be −70 and +5 mV, respectively, which attributes high linear charge density to DNA and considerably low charge density to the protein. In salt-free environment, DNA and GA molecules are expected to interact strongly through Coulomb interactions and form intermolecular complexes. Figure 1 data reveal a considerable decrease in the size of the DNA–GA complex as the protein concentration was varied in the range 0 to 0.05% (w/v). This clearly indicated DNA–GA binding through electrostatic interactions, which was evident from the fact that the charge on the DNA reduced by close to 25% during this interaction (Figure 1). In our experiment, however, a large amount of GA was required for the occurrence of condensation and neutralization of DNA. This phenomenon can be understood as follows. First, because of the high charge ratio (DNA:GA = 16:1), more of GA is required to bind and neutralize DNA backbone. Second, because of the large and random coil structure of GA, DNA will feel steric hindrance while attaching to the incoming GA molecule; regardless, the surface patch binding[5,7] of GA to DNA backbone was realized. Gelatin A is a polyampholyte molecule containing both positive and negatively charged residues.[24] Therefore, the positively charged segments of the chain will preferentially bind to DNA. Such interaction of DNA ($R_{DNA} \approx 140$ nm) with GA ($R_{GA} \approx 55$ nm) was responsible for reducing the size of DNA–GA complex, $R_{complex}$. It is to be noted that the stiffness of DNA molecule was reduced as more and more GA molecules bound to it because of the concomitant reduction in the electrostatic persistence length of DNA. This interaction, which was electrostatic in nature, was supported by ζ potential data that depict partial charge neutralization of DNA–GA complex upon the addition of GA in this concentration region. This has been referred to as primary binding.

3.4. Growth of Complex (0.05 < C_{GA} < 0.1% (w/v)). Compact complexes that are partially charge-neutralized as stated in the previous section continued to attract more GA for further binding, and as a consequence the size of complex increased until complete charge neutralization of complex was achieved (secondary binding). The size of the complex, $R_{complex}$ started to increase from 60 nm to a maximum size of $R_{complex} \approx$ 180 nm with the increase in C_{GA}, as is clear from DLS data (Figure 1). This increase in size of complex got saturated at $C_{GA} \approx 0.1\%$ (w/v), which was also the charge neutralization point (ζ potential = 0) and maximum turbidity loci. Interestingly, the viscosity data revealed the same information; notice the change in slope of the relative viscosity profile at $C_{GA} \approx 0.08\%$ (w/v) in Figure 2. Therefore, the DLS and viscosity data collectively defined the region for secondary binding.

3.5. Complex Coacervation and Overcharging ($C_{GA} \geq$ 0.1% (w/v)). In the GA concentration range 0.05 to 0.1% (w/v),

dx.doi.org/10.1021/jp3073798 | J. Phys. Chem. B 2012, 116, 13192–13199

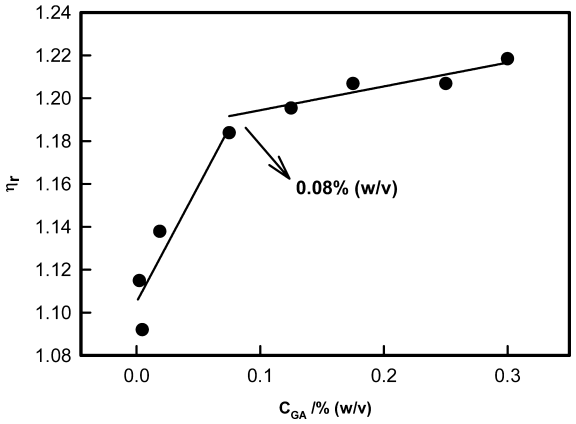

Figure 2. Variation of relative viscosity as a function of C_{GA}. Notice the change in slope at $C_{GA} \approx 0.1\%$ (w/v).

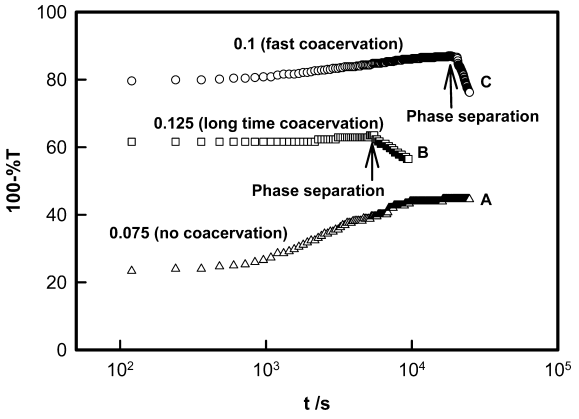

Figure 3. Variation of turbidity as function of time for three GA concentrations: (A) below, (B) above, and (C) at C_{GA} = 0.1% w/v (neutralization point). Note that for sample A coacervation is absent.

the size of the DNA−GA complex was found to increase considerably while the ζ potential value reduced and approached zero, clearly indicating charge neutralization of the complex. Correspondingly, the turbidity increased and revealed a maximum at C_{GA} = 0.1% (w/v), followed by a sharp decrease in its value for C_{GA} > 0.1% (w/v). Thus, the ζ potential and turbidity profiles carried the distinctive signature[2−4] of complex coacervation at and after C_{GA} = 0.1% (w/v). Overcharging of the DNA−GA complex was seen beyond the charge neutralization point, which will be discussed in the next section. The formation of charge-neutralized intermolecular complexes is known to precede complex coacervation transition, which has been observed in a wide variety of interacting polyelectrolyte systems.[1−10]

It is expected that beyond the charge-neutralization point, if more complementary polyelectrolyte is added then further binding is not favored and the ζ potential would remain same. However, many theoretical predictions made in the past show that even after charge neutralization oppositely charged macroions can bind to the charge-neutralized complex and render them overcharged. This overcharging phenomena is energetically favored.[13,17] In our case, turbidity of solution and size of complex decreased, whereas ζ potential showed overcharging, which may owe its origin to nonuniform binding of GA to DNA in the process of forming complex. Further increase in the concentration of GA beyond C_{GA} = 0.1% (w/v) led to the formation of oversized and unstable complexes, which yielded liquid−liquid phase separation. (Note the sharp decline in the value of turbidity for C_{GA} > 0.1% (w/v).) The process of complex coacervation was poorly seen below C_{GA} = 0.1% (w/v); however, coacervation was maximum at the neutralization point and remained weak for higher C_{GA} values due to the overcharging of complexes that had ζ potential of about +15 mV. This phenomenon is supported by data shown in Figure 3, where it is shown that below the charge neutralization point no coacervation existed, while dynamics of coacervation was maximum close to the neutralization point. Beyond the neutralization point dynamics of coacervation was again slowed due to overcharging phenomena. The overcharged complexes in solution, because of their excess positive charge, tried to repel each other and remained in stable dispersion for a sufficient amount of time, thus inhibiting coacervation. However, at longer time, these undergo phase separation, as indicated in Figure 3.

3.6. Modeling of DNA−GA Binding. In the interaction model conceptualized below, we make the following assumptions: (i) DNA molecule is a sequence of n-equally spaced nucleotides of size r_1, and each of these carry charge of $-Q$ units; (ii) the Gelatin A molecule is treated as a counterion of charge $+q$ and size r_2; and (iii) all potentials other than electrostatic and van der Waal interactions are ignored. Figure 4 describes this

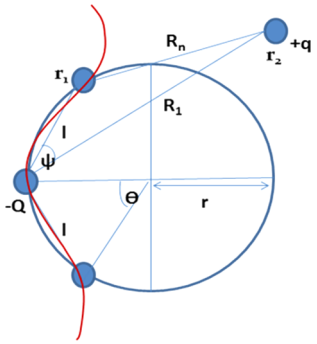

Figure 4. Model of DNA and GA interaction. Nucleotides shown as small filled circles are placed on the circumference of a circle of radius r. Inter nucleotide spacing is l, and its polar location is θ. GA molecule is shown as a counterion. R_n is the distance between GA and the nth nucleotide of DNA, $-Q$ is charge on nucleotide, $+q$ is charge on GA, and r_1 and r_2 are radii of nucleotide and GA molecule, respectively.

situation clearly where the nucleotides are localized on the surface of a semicircle of radius r and the spatial location of the nucleotides is defined through angles θ and ψ, and position coordinates $\{R_1...R_n\}$. Under these assumptions, the interaction potential ϕ between a nucleotide and the counterion can be written as[25]

$$\phi = -qQ\frac{\exp(-\kappa R_1)}{R_1} - \frac{A}{6}\left[\frac{2r_1r_2}{2(r_1+r_2)(R_1-(r_1+r_2))+(R_1-(r_1+r_2))^2} + \frac{2r_1r_2}{4r_1r_2+2(r_1+r_2)(R_1-(r_1+r_2))+(R_1-(r_1+r_2))^2} + \ln\frac{2(r_1+r_2)(R_1-(r_1+r_2))+(R_1-(r_1+r_2))^2}{4r_1r_2+2(r_1+r_2)(R_1-(r_1+r_2))+(R_1-(r_1+r_2))^2}\right] \quad (4)$$

where the first term on RHS is electrostatic contribution and other three terms account for van der Waal forces with A defined as Hamaker constant. Here we have included the individual

dx.doi.org/10.1021/jp3073798 | J. Phys. Chem. B 2012, 116, 13192−13199

contribution of electrostatic and van der Waal forces to account for DNA−GA complex formation.

The negatively charged nucleotides of DNA are arranged in a semicircle at an equal spacing l and angle θ between them. The number of nucleotides taken for our modeling was 11, and inclusion of a greater number of nucleotides did not affect the overall potential. This may be because the GA molecule approaching DNA with a higher number of nucleotides was not able to see the potential arising from far off nucleotides. A GA molecule having $+q$ charge approaches the DNA molecule at an angle ψ, as shown in Figure 4.

(i). Primary Binding (C_{GA} < 0.05% w/v). As GA molecule approaches DNA, primary intermolecular electrostatic binding between GA and DNA occurs that tries to neutralize the DNA charge; therefore, electrostatic persistence length of DNA decreases. As more GA molecules bind, this decrease progresses in a cooperative way, giving rise to condensation of the DNA−GA complex. Therefore, effective hydrodynamic radius of DNA, $R_{DNA} \approx 140$ nm, in the presence of GA, reduces to ∼60 nm at C_{GA} = 0.05% (w/v). In this region, the solution turbidity remained largely invariant and the ζ potential of dispersed moieties decreased from −70 to −50 mV, indicating partial charge neutralization of DNA due to its surface-selective binding with GA molecules. This generated small but stable soluble complexes through a process that we refer to as primary binding.

The existence of primary binding and the formation of stable small DNA−GA complexes was energetically favored when electrostatic screening was increased. This phenomenon can easily be understood on the basis of results shown in Figure 5,

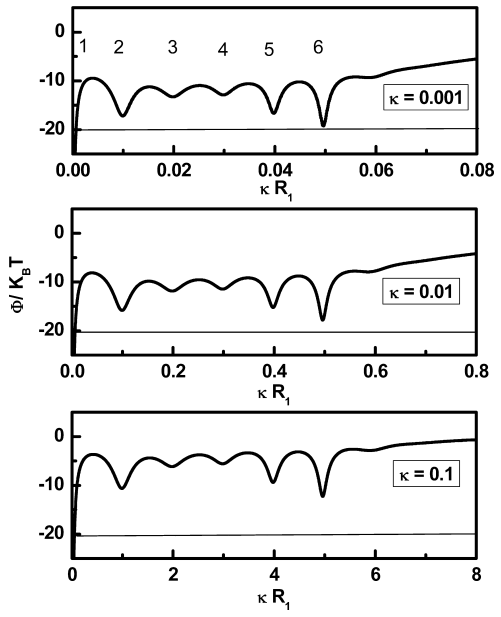

Figure 5. Interaction potential as a function of DNA−GA intermolecular separation R_1 shown for Debye screening parameters κ = 0.1, 0.01 and 0.001.

which clearly show the preferential formation of smaller size complexes with increasing electrostatic screening. In Figure 5, the independent variable (R_1) is the intermolecular distance between DNA and GA, where there is possibility of formation of stable complexes. As electrostatic screening was induced due to increasing concentration of GA, the depth of potential decreased at higher R_1 values, but the system preferred lower R_1 configurations that give rise to the formation of smaller complexes.

In Figure 5 with screening constant κ = 0.001, the sixth potential has an order of 20, whereas the fifth potential has an order of 18. When the screening constant is increased to κ = 0.01, sixth potential achieves a value of 18 and the fifth potential achieves a value of 15. A similar kind of behavioral changes was seen for other potentials. These potentials further decreased for κ = 0.1 (qualitatively refers to our experimental condition). Moreover, in our case, we are treating GA as counterion and increasing screening constant simply implies that we are introducing more GA for neutralizing DNA. This clearly stipulates that with increasing screening constant (addition of more GA), the tendency to form larger complexes decreases and the system will be selectively driven toward first potential to form smaller complexes. This explains the salient features of primary binding.

(ii). Dominance of van der Waals Forces (0.05 < C_{GA} < 0.1% w/v). After condensation of the DNA−GA complex in region C_{GA} < 0.05% w/v, further electrostatic attraction was unfavorable due to substantial screening of DNA charge by GA counterions. In the absence of Coulombic interactions, van der Waals attractive forces will be dominant between the partially charge neutralized DNA−GA complex and free GA molecules. This attractive force will further drive the binding process, causing the size of these soluble complexes to increase until maximum sustainable size is realized. In this region, the turbidity increased sharply, the ζ potential of moieties reduced significantly (−50 to 0 mV), and their size grew three-fold from 60 to 180 nm. (See Figure 1.) These characteristic signatures indicated secondary binding between DNA−GA complex and the existence of free GA molecules.

The feasibility of the aforesaid interaction phenomena is energetically favorable, as it is clearly observed from Figure 6, which shows that as the size of the complex formed at the nucleotide site increases, the formation of larger complexes is facilitated.

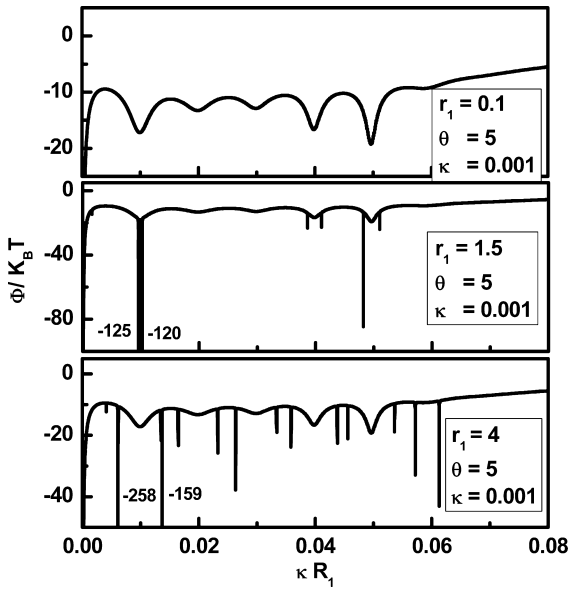

Figure 6. Interaction potential as a function of intermolecular DNA−GA separation R_1 shown for Debye screening parameter κ = 0.001 with varying size of complex at nucleotide site.

dx.doi.org/10.1021/jp3073798 | J. Phys. Chem. B 2012, 116, 13192−13199

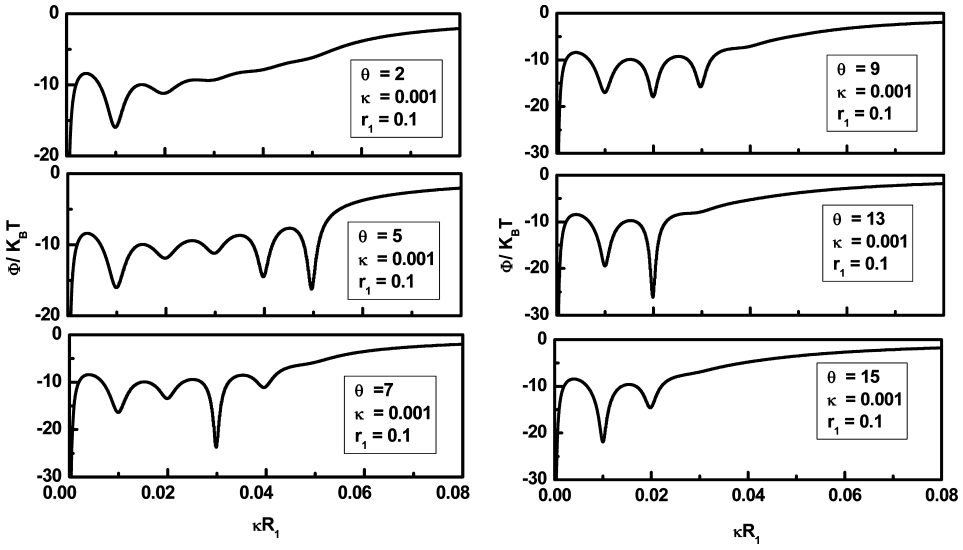

Figure 7. Interaction potential as a function of intermolecular DNA−GA separation R_1 for a given Debye parameter κ shown for different curvatures of DNA.

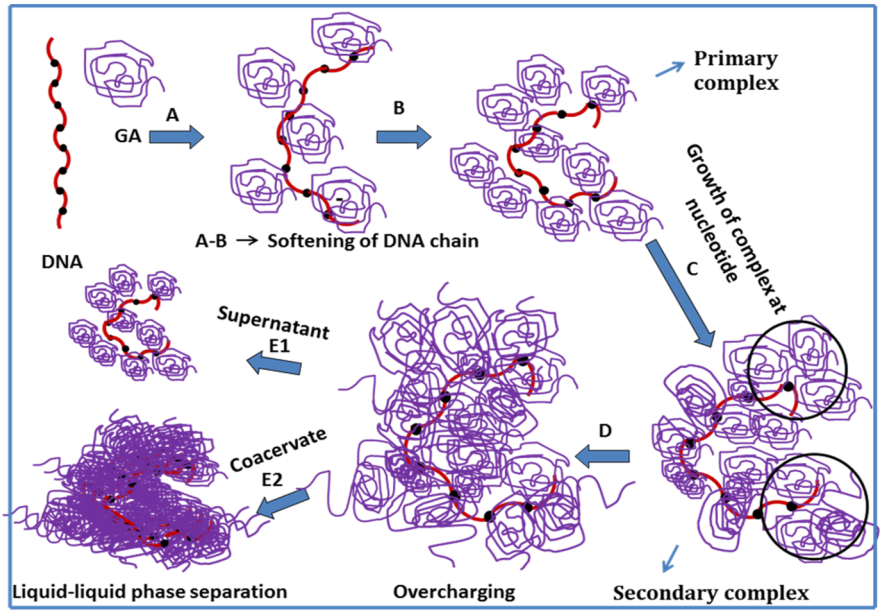

Figure 8. Schematics of DNA−GA complex formation and coacervation.

Here we focus only on the changes due to van der Waal forces, neglecting the effect of electrostatic interaction. Thus, the model assumes a fixed electrostatic screening constant and emphasizes on changing the radius of the complex formed at the location of the nucleotides. It was clearly observed that as the size of complexes at nucleotide site increased, potential at farther R_1 was favored and so the probability to form larger complexes was more likely.

(iii). Effect of Stiffness of DNA on Complex Formation. A typical GA molecule approaching DNA will see numerous potentials due to large number of nucleotides of DNA, but the effective potential that GA molecule will see depends on the local curvature of DNA (its stiffness). If this is too small, then the incoming GA molecule will see as if all nucleotides are located at a fixed place in space, and thus it will see a smaller number of potentials. If the curvature of DNA is large enough, then nucleotides will be found at larger spatial separations, and the GA molecule will not be able to see all potentials simultaneously. Hence, an optimum curvature of DNA is responsible for GA to see a reasonable number of favorable potentials, as is illustrated in Figure 7, and produce stable complexes. Note that the $\theta = 5°$ angle of approach corresponds to visualization of maximum number of potentials.

(iv). Schematic Depiction of DNA−GA Binding. The above model depicts that initial softening of the DNA strand is occurring due to a decrease in electrostatic persistence length of DNA as GA approaches DNA to form primary complex. This complex then grows in size until full charge neutralization of DNA is realized. The neutralized complex can, however, sustain a larger number of GAs (which is energetically favored), which leads to overcharging of the resultant complex, but because this complex is too large in size, it will not remain in stable dispersion and the process of liquid−liquid phase separation (complex coacervation) ensues. This is the first experimental report of

dx.doi.org/10.1021/jp3073798 | J. Phys. Chem. B 2012, 116, 13192−13199

observation of overcharged complexes, although the same was previously predicted.[16,17]

3.7. Model for Overcharging. From Figure 1 it was observed that even after charge neutralization of DNA by GA at C_{GA} = 0.1% (w/v) and formation of soluble secondary complexes more protein could bind to these complexes with unique overcharge attributes. The presence of the additional GA molecules in the secondary complexes was responsible for reversing the charge state from negative to positive and creating overcharging. The possible reason for this overcharging is nonuniform distribution of charge on GA that allows surface-selective binding of protein to pre-existing secondary DNA−GA complexes. This binding phenomenon that gave rise to overcharging was modeled as follows.

Let $-Q$ be the charge on DNA as macro ion and $+q$ be the charge on GA as counterion. It will be assumed that average distance between the counterions is $\bar{b}$ and the average distance between macro ion and counterion is $\bar{a}$. The model is illustrated in Figure 9.

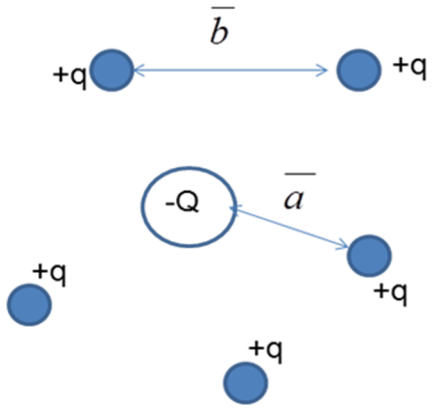

Figure 9. Model for interaction between DNA macro ion and GA counterions.

Using pairwise interaction, the average macro ion−counterion and counterion−counterion interaction energy for $N = N_c$ number of counterions, where N_c denotes the number of counterions needed to neutralize the macro ion, is written as[26,27]

$$\overline{E_{N_c}} = \left(\frac{-QqN_c}{\bar{a}}\right) + q^2\left(\frac{N_c(N_c-1)}{2\bar{b}}\right) \quad (5)$$

Similarly, average macro ion-counterion and counterion-counterion interaction energy for $N = N_c + n$ number of counterions, where n denotes number of counterions needed to overcharge the macro ion is written as[26,27]

$$\overline{E_N} = \left(\frac{-QqN}{\bar{a}}\right) + q^2\left(\frac{N(N-1)}{2\bar{b}}\right) \quad (6)$$

where $-Q$ and q are charge calculated from ζ potential. Energy difference $\Delta E = \overline{E}_N - \overline{E}_{N_c}$ plotted against n is shown in Figure 10, which suggests that increasing the counterion beyond neutralization provides stability to the system and overcharging can be observed in these complexes. Overcharging is further increased if the average counterion−counterion separation is larger than the average macro ion−counterion separation.

The number of excess counterions n_{min} required to produce an overcharged complex can be determined from the loci of the minima of the free-energy plot shown in Figure 10. This Figure

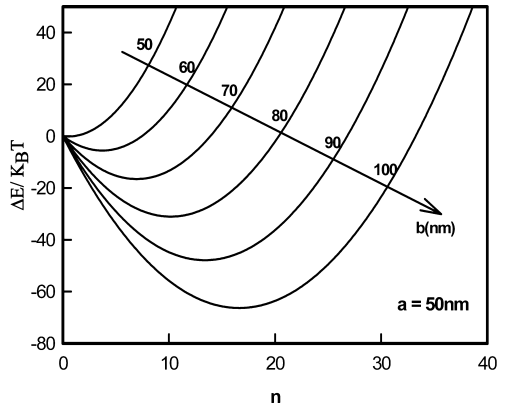

Figure 10. Variation of $\Delta E/K_BT$ versus n for different counterion−counterion distances.

shows the variation of n_{min} with respect to counterion−counterion separation. Interestingly, a plot of n_{min} versus b yields the cubic power-law dependence ($n_{min} \approx b^{2.83}$) between them (Figure 11). This can be understood as follows: n_{min} corresponds

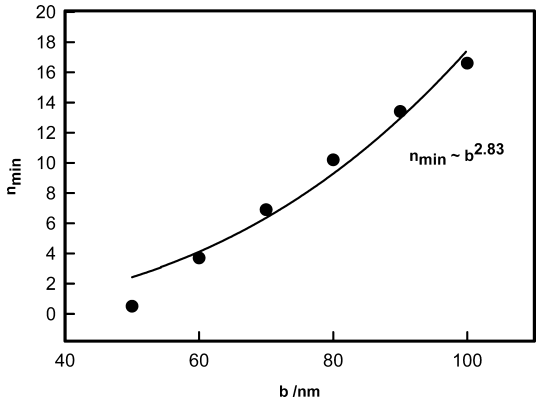

Figure 11. Variation of minimum number of counterions required for overcharging versus counterion−counterion separation.

to extra charge and b^3 corresponds to the volume existing between counterions. Therefore, for higher overcharging, separation between counterions must increase. Increased separation reduces electrostatic screening of the macroion, and so more counterions will be required to achieve charge neutralization. However, the precise cause for this is not understood at this point.

4. CONCLUSIONS

We have discussed complexation of DNA and Gelatin A having comparable molecular weight. The complexation mechanism can be broadly divided into two parts, that is, before and after the charge-neutralization point. Prior to neutralization, the initial size of complex decreased due to electrostatic screening of DNA and, as a consequence, decrease in its electrostatic persistence length. Following this, the size of the DNA−GA complex increased to further charge neutralize the complex. Beyond the neutralization point, coacervation and interesting overcharging behavior of the complexes were noticed. Despite enhancing the coacervation after the charge-neutralization point, overcharging played an important role in suppressing the dynamics of coacervation. We modeled the behavior of complex formation before charge neutralization was achieved by using only electrostatic and van

Table 1. Comparison of Binding Leading to Complex Coacervation in Diverse Systems[a]

Sl no.	properties	GA + GB[8,28]	GA + L[29]	GA + DNA[thiswork]
1	binding type	protein−protein	protein−colloid	protein−DNA
2	binding ratio[b]	1.5 (GA/GB)	4.7 (GA/L)	20 (GA/DNA)
3	persistence length	10 nm (GA); 2 nm (GB)	10 nm (GA); 3 nm (L)	10 nm (GA); 50 nm (DNA)
4	ζ potential ratio	2 (GB/GA)	5 (L/GA)	16 (DNA/GA)
5	overcharging	absent	absent	present
6	pH_c	6.5	7.2	6.0
7	optical nature[c]	clear	clear	turbid
8	coacervation	electrostatic	electrostatic	electrostatic and vdW

[a]GA, GB, and L represent Gelatin A, Gelatin B, and Laponite, respectively. [b]Represents optimum binding ratio (molecule/molecule). [c]At pH_c.

der Waal forces. The overcharging phenomenon was modeled and showed the feasibility of binding of GA to pre-existing DNA−GA complexes, leading to the overcharging post charge neutralization. It is pertinent to note that the effect of heterogeneous surface selective binding of GA to DNA−GA charged-neutralized complex cannot be ruled out. It was felt imperative to compare three identical systems where complex coacervation following intermolecular binding has been reported in the past.[8,28,29] This is illustrated in Table 1. Interestingly, overcharging was observed only in the case of the protein−nucleic acid system, which clearly implies that this phenomenon owes its origin to the high charge density of the nucleic acid and its surface selective binding with a low charge density protein. In summary, it needs to be emphasized that overcharging in biopolymer complexation appears to be more common than previously thought, which has a profound effect on molecular biophysics. This definitely calls for more systematic study and examination of protein−protein and protein−nucleic acid interactions.

■ ASSOCIATED CONTENT

Supporting Information

Agarose gel electrophoresis for DNA and SDS-PAGE for Gelatin A (bloom 300) panels. This material is available free of charge via the Internet at http://pubs.acs.org.

■ AUTHOR INFORMATION

Corresponding Author

*E-mail: bohi0700@mail.jnu.ac.in. Tel: +91 11 2670 4637. Fax: +91 11 2674 1837.

Notes

The authors declare no competing financial interest.

■ ACKNOWLEDGMENTS

N.A. acknowledges receiving a Senior Research Fellowship from Council for Scientific and Industrial Research, India.

■ REFERENCES

(1) Bungenberg de Jong, H. G. In *Colloid Science*; Kruyt, H. R., Ed.; Elsevier Academic Press: New York, 1949; Ch. III.
(2) Tsuchida, E.; Abe, K. *Intermacromolecular Complexes*; Springer: Heidelberg, 1982.
(3) Park, J. M.; Muhoberac, B. B.; Dubin, P. L.; Xia, J. *Macromolecules* **1992**, *25*, 290−295.
(4) Kaibara, K.; Okazaki, T.; Bohidar, H. B.; Dubin, P. L. *Biomacromolecules* **2000**, *1*, 100−107.
(5) Gupta, A.; Bohidar, H. B. *J. Phys. Chem. B* **2007**, *111*, 10137−145.
(6) Singh, S. S.; Aswal, V. K.; Bohidar, H. B. *Int. J. Biol. Macromol.* **2007**, *41*, 301−307.
(7) Boral, S.; Bohidar, H. B. *J. Phys. Chem. B* **2010**, *114*, 12027−12035.
(8) Tiwari, A.; Bindal, S.; Bohidar, H. B. *Biomacromolecules* **2009**, *10*, 184−189.
(9) Burgess, D. J. *J. Colloid Interface Sci.* **1990**, *140*, 227−238.
(10) Smith, A. E. *Nature* **1967**, *214*, 1038−1040.
(11) Mrevlishvili, G. M.; Svintradze, D. V. *Int. J. Biol. Macromol.* **2005**, *35*, 243−245.
(12) Kaya, M.; Toyama, Y.; Kubota, K.; Nodasaka, Y.; Ochiai, M.; Nomizu, M.; Nishi, N. *Int. J. Biol. Macromol.* **2005**, *35*, 39−46.
(13) Nguyen, T. T.; Shklovskii, B. I. *J. Chem. Phys.* **2001**, *115*, 7298−7308.
(14) Poverenny, A. M. *Connective Tissues in Health and Diseases "Nauka*; Novosibirsk: USSR, 1968.
(15) Kitamura, H.; Iwamoto, N. S.; Sakai, N.; Tokura, S.; Nishi, N. *Int. J. Biol. Macromol.* **1997**, *20*, 241−250.
(16) Zhang, R.; Shklovskii, B. I. *Physica A* **2005**, *352*, 216−238.
(17) Gurovitch, E; Sens, P. *Phys. Rev. Lett.* **1999**, *82*, 339−342.
(18) Landau, L. D.; Lifshitz, E. M. *Fluid Mechanics*, Pergamon: New York, 1987.
(19) Micka, U.; Kremer, K. *Europhys. Lett.* **1997**, *38*, 279−284.
(20) Benoit, H.; Doty, P. *J. Phys. Chem.* **1953**, *57*, 958−963.
(21) Eisenberg, H. *Acc. Chem. Res.* **1987**, *20*, 276−282.
(22) Minagawa, K.; Matsuzawa, Y.; Yoshikawa, K.; Matsumoto, M.; Doi, M. *FEBS Lett.* **1991**, *295*, 67−69.
(23) Frisch, H. L.; Fesciyan, S. *J. Polym. Sci., Polym. Lett.* **1979**, *17*, 309−315.
(24) *Merck Index*, 12th ed.; Budavari, S. Ed.; Merck: Whitehouse Station, NJ, 1996; Vol. *742*, p 4388.
(25) Bordi, F.; Sennato, S.; Truzzolillo, D. *J. Phys.: Condens. Matter* **2009**, *21*, 203102.
(26) Shklovskii, B. I. *Phys. Rev. E* **1999**, *60*, 5802−5811.
(27) Mukherjee, A. K.; Schmitz, K. S.; Bhuiyan., L. B. *Langmuir* **2003**, *19*, 9600−9612.
(28) Gupta, A.; Mohanty, B.; Bohidar, H. B. *Biomacromolecules* **2005**, *6*, 1623−1627.
(29) Pawar, N.; Bohidar, H. B. *J. Polym. Sci., Part B: Polym. Phys.* **2010**, *48*, 555−565.